doi:10.1093/brain/awp174 Brain 2009: 132; 2239–2251 | 2239

BRAIN
A JOURNAL OF NEUROLOGY

Delayed post-ischaemic neuroprotection following systemic neural stem cell transplantation involves multiple mechanisms

Marco Bacigaluppi,[1,2,3,*,†] Stefano Pluchino,[2,3,*,†] Luca Peruzzotti Jametti,[2,3,†] Ertugrul Kilic,[1] Ülkan Kilic,[1] Giuliana Salani,[2,†] Elena Brambilla,[2] Mark J. West,[4] Giancarlo Comi,[2,3] Gianvito Martino[2,3,*] and Dirk M. Hermann[1,5,*]

1 Department of Neurology, University Hospital Zurich, Frauenklinikstrasse 26, CH-8091 Zurich, Switzerland
2 Neuroimmunology Unit-DIBIT2 and Institute of Experimental Neurology, San Raffaele Scientific Institute, Via Olgettina 58, I-20132 Milan, Italy
3 Department of Neurology and Neurophysiology, San Raffaele Scientific Institute, Via Olgettina 58, I-20132 Milan, Italy
4 Institute of Anatomy, University Park, DK-8000 Aarhus, Denmark
5 Department of Neurology, University Hospital, University of Duisburg-Essen, Hufelandstrasse 55, D-45122 Essen, Germany

*These authors contributed equally to this work.

†Present address: CNS Repair Unit-DIBIT2, and Institute of Experimental Neurology,
San Raffaele Scientific Institute,
Via Olgettina 58,
I-20132 Milan,
Italy

Correspondence to: Prof. Dr Dirk M. Hermann,
Chair of Vascular Neurology,
Dementia and Ageing Disorders,
Department of Neurology,
University Hospital Essen,
Hufelandstr. 55,
D-45122 Essen,
Germany
E-mail: dirk.hermann@uk-essen.de

Recent evidence suggests that neural stem/precursor cells (NPCs) promote recovery in animal models with delayed neuronal death via a number of indirect bystander effects. A comprehensive knowledge of how transplanted NPCs exert their therapeutic effects is still lacking. Here, we investigated the effects of a delayed transplantation of adult syngenic NPCs—injected intravenously 72 h after transient middle cerebral artery occlusion—on neurological recovery, histopathology and gene expression. NPC-transplanted mice showed a significantly improved recovery from 18 days post-transplantation (dpt) onwards, which persisted throughout the study. A small percentage of injected NPCs accumulated in the brain, integrating mainly in the infarct boundary zone, where most of the NPCs remained undifferentiated up to 30 dpt. Histopathological analysis revealed a hitherto unreported very delayed neuroprotective effect of NPCs, becoming evident at 10 and 30 dpt. Tissue survival was associated with downregulation of markers of inflammation, glial scar formation and neuronal apoptotic death at both mRNA and protein levels. Our data highlight the relevance of very delayed degenerative processes in the stroke brain that are intimately associated with inflammatory and glial responses. These processes may efficaciously be antagonized by (stem) cell-based strategies at time-points far beyond established therapeutic windows for pharmacological neuroprotection.

Received December 17, 2008. Revised May 15, 2009. Accepted May 21, 2009

Keywords: stroke; neural stem/precursor cells; transplantation; inflammation; gliosis

Abbreviations: CC = corpus callosum; CNS = central nervous system; dpt = days post-transplantation; i.v. = intravenously; LDF = laser Doppler flow; MCAO = middle cerebral artery occlusion; NPCs = neural stem/precursor cells

Introduction

According to current pathophysiological concepts, the structural histological injury following stroke evolves within several hours to up to 3–4 days, depending on the duration and severity of the ischaemic event (Namura *et al*., 1998; Hata *et al*., 2000; Hermann *et al*., 2001). During that time, secondary energy failure develops in the ischaemic penumbra via multiple mechanisms including excitotoxicity, lactacidosis and peri-infarct depolarizations (Hossmann, 2006). In the ischaemic border zone surrounding the evolving infarct, inflammatory responses and apoptotic programs are activated in this phase that further contribute to injury development (Dirnagl *et al*., 1999; Hermann *et al*., 2001; Hossmann, 2006). Following the acute stroke phase, the tissue undergoes substantial matrix remodelling that results in (astro)glial scar formation, which is widely regarded as a major hampering factor for tissue repair and regeneration (Fawcett and Asher, 1999; Nedergaard and Dirnagl, 2005; Yiu and He, 2006).

Several lines of evidence suggest that the structural and functional changes in the ischaemic boundary zone are of key importance for the final stroke outcome (Witte, 1998; Nudo, 1999). This might imply that therapies favouring endogenous tissue repair and/or remodelling may have realistic chances of success also when applied beyond established time-windows of tissue protection, which in the case of thrombolytics in humans are in the range of 3–6 h (Hacke *et al*., 2008). The pathophysiology of this second phase is highly heterogeneous in time and space, and the underlying mechanisms are still poorly understood (Lee *et al*., 2008). There is common sense that classical pharmacological strategies aiming at improving neuronal survival are no more useful at this latter stage (Zivin, 1998).

Neural stem/precursor cells (NPCs) display remarkable therapeutic plasticity upon transplantation in experimental conditions mimicking central nervous system (CNS) diseases, by adapting their fate and function(s) to specific environments under pathological conditions (Martino and Pluchino, 2006). Key functions such as the replacement of neural cells (Pluchino *et al*., 2003; Karimi-Abdolrezaee *et al*., 2006) and the delivery of therapeutic gene(s) (Lee *et al*., 2007) have been recently challenged by intrinsic bystander capacities, mainly exerted by undifferentiated NPCs, releasing at the site of tissue damage, a milieu of immune-regulatory molecules that is temporally and spatially orchestrated by specific environmental needs (Pluchino *et al*., 2005). Furthermore, NPCs synergize with local immune (e.g. T cells and microglia) (Ziv *et al*., 2006) and CNS resident (e.g. endothelial cells, astrocytes) cells (Pluchino *et al*., 2005), modulating the focal release of stem cell regulators and—in turn—promoting functional recovery from CNS injuries. The molecular and cellular mechanisms mediating such bystander effects still remain to be characterized.

The brain repair potential of NPCs acutely transplanted in stroke-like conditions—both ischaemic and haemorrhagic—has solid pre-clinical evidence (Bliss *et al*., 2007; Lee *et al*., 2008). Thus, the issue as whether (and how) NPCs also modulate delayed cerebral responses after stroke has important therapeutic relevance that should be clarified in order to correctly adjust cell-based therapies to tissue needs. Here, we report the capacity of the post-acute transplantation of syngenic adult NPCs injected intravenously (i.v.) at 72 h post-ischaemia to induce functional neurological recovery in mice with transient middle cerebral artery occlusion (MCAO). Histological analysis revealed a so far unreported very delayed neuroprotective effect that began to evolve at 10 days post-transplantation (dpt) and was even more pronounced at 30 dpt. Molecular biological and histochemical studies revealed profound anti-inflammatory, glial scar-inhibitory and anti-apoptotic effects of NPCs, which were responsible for the neuroprotection and the functional improvements.

Materials and Methods

Intraluminal MCAO

Details on the study design are presented in Supplementary Fig. 1. Forty-five minutes of MCAO were induced in adult male 8- to 10-week old (weight 20–25 g) C57Bl/6 mice (Harlan Nossan, Netherlands), as previously described (Hata *et al*., 2000; Hermann *et al*., 2001). Experiments were performed at the University Hospital Zurich according to the National Institutes of Health guidelines for the care and use of laboratory animals with approval of local government authorities (Cantonal Veterinary Office, ZH 169/2005). During the experiments, up to 15 min after reperfusion, laser Doppler flow (LDF) was monitored above the core of the middle cerebral artery territory. Further information is provided in the Supplementary materials and Methods section.

NPC preparation and transplantation

Adult neurospheres were generated from the subventricular zone of 8-month-old C57Bl/6 mice, as described (Pluchino *et al*., 2005), and i.v. delivered at 72 h after reperfusion via the tail vein. Further information is provided in the Supplementary Materials and Methods section.

Behavioural analysis

Modified neurological severity score (mNSS) was evaluated at baseline, on the day of transplantation prior to cell delivery, on a daily basis between 1 and 11 dpt, and then every second to fourth day up to 30 dpt. Grip strength test was performed at baseline, at 3 days after MCAO, immediately before cell transplantation, and at 3, 10, 20 and 30 dpt. Behavioural tests were performed during the light phase of the circadian cycle beginning 4 h after lights on. Further

information is provided in the Supplementary Materials and Methods section.

Tissue pathology

At sacrifice, mice were transcardially perfused with 4% paraformaldehyde and brain, liver, spleen, kidneys and lungs were removed and processed for tissue histopathology as frozen tissue samples (Pluchino *et al*., 2005). Further information is provided in the Supplementary Materials and Methods section.

Stereological analysis

In the striatum, cell numbers for NeuN, Darpp-32 and D2R were quantified according to the optical fractionator method with the assistance of the Stereo Investigator v 3.0 software (MicroBrightField, Inc., Colchester, VT, USA) (West *et al*., 1991).

Estimates of the length of capillaries (threshold smaller than 8 μm) were made throughout the striatum (ischaemic and contralateral) on CD 31 stained sections with the use of virtual isotropic hemispherical probes (radius = 22 μm) on the Stereo Investigator v 3.0 software (MicroBrightField) (Mouton *et al*., 2002). Further information is provided in the Supplementary Materials and Methods section.

Real-time PCR

Real-time quantitative PCR was performed using pre-developed Taqman™ Assay Reagents on an ABI Prism™ 7700 Sequence Detection System (Applied Biosystems, Carlsbad, California, USA) according to the manufacturer's protocol. Further information is provided in the Supplementary Materials and Methods section.

Statistical analysis

For statistical analyses, we used a standard software package (GraphPad Prism version 4.00). To test the treatment effect on each of the behaviour scores, behavioural tests were evaluated by means of repeated measurement analysis of variance (ANOVA). Whenever a treatment by time interaction or treatment effect was present at the 0.05 level, a *post hoc* analysis was done by Bonferroni test. Histological data were evaluated by unpaired two-tailed *t*-tests. Gene expression analyses were evaluated by two-tailed *t*-tests and by two-way ANOVA followed by Bonferroni test.

Results

Progressive improvement of neurological deficits after NPC transplantation

Mice subjected to transient MCAO (Hata *et al*., 2000) were injected i.v. with syngenic subventricular zone-derived green fluorescent protein $(GFP)^+$ adult NPCs (1.0×10^6 cells per mouse) at 72 h after reperfusion, following a delayed (post-acute) cell transplantation scheme (Pluchino *et al*., 2003, 2005). Post-randomization analysis of the LDF measurements, weight loss and neurological deficit scores (mNSS and grip strength test) both prior to the induction of cerebral ischaemia (−3 dpt) and before treatment (Day 0) did not show any differences between the groups (Fig. 1A–D).

Neurological performance was monitored all along the follow-up until 30 dpt. Indeed, remarkable development of neurological deficits was observed upon MCAO in both groups of mice. NPC-transplanted MCAO mice showed a progressively enhanced recovery of motor skills in the mNSS—starting to be significant from 18 dpt onwards ($P \leqslant 0.05$)—as compared with sham-treated controls. This improvement was also reflected by stronger grip strength in the right paretic forepaw (Fig. 1 C–D). The grip strength in the left non-paretic forepaw did not differ between the groups (data not shown).

Accumulation and long-term persistence of transplanted NPCs in the ischaemic boundary zone

To assess the distribution and the identity of i.v.-injected NPCs in the ischaemic brain, a detailed morphometric analysis was carried out at 3, 10 and 30 dpt in the brain and in peripheral tissues such as spleen, liver, kidneys and lungs. Only 0.09% of injected NPCs were detected in the brain by 3 dpt and the cells accumulated in both hemispheres, ipsilateral and contralateral to the stroke (3.47 ± 0.96 and 4.25 ± 1.6 cells/mm^3, respectively). At later time-points, NPCs were detected exclusively in the ischaemic hemisphere. As such, the number of NPCs increased by 5.5-fold at 10 dpt (0.23% of transplanted NPCs, 19.4 ± 4.87 cells/mm^3, $P \leqslant 0.05$ compared with 3 dpt), the majority GFP^+ NPCs accumulating in the ischaemic boundary zone. At 30 dpt numbers of NPCs remained similarly high (0.28% of transplanted NPCs, 20.5 ± 4.2 cells/mm^3, $P \leqslant 0.05$ compared with 3 dpt). Sham-treated ischaemic mice did not display any immunoreactivity for GFP, neither in the brain nor in peripheral tissues (Fig. 2A and B).

To characterize the proliferation and differentiation capacity of transplanted NPCs, different immunohistochemical stainings were performed. Twenty-five percent of GFP^+ cells at 3 dpt expressed the Ki67 antigen, a molecular marker that is expressed exclusively in proliferating cells during the late G_1, S, G_2 or M phase of the cell cycle. The great majority of NPCs within the brain at 3 and 10 dpt did not express any of the major antigens of the neural lineage, such as glial fibrillary acidic protein, doublecortin (Dcx), microtubule-associated protein (MAP)-2 and the oligodendroglial transcription factor (Olig 2) (data not shown). The percentage of $Ki67^+$ NPCs decreased at later time-points (6.9% at 10 dpt, 0.8% at 30 dpt), whereas the majority of cells still remained undifferentiated. Even at 30 dpt, only 4.4% and 0.8% of i.v.-injected NPCs at 30 dpt expressed Olig2 and doublecortin, respectively (Fig. 2C–F).

Similarly to what others and we have shown in experimental autoimmune encephalomyelitis, NPCs detected in the ischaemic boundary zone established anatomical interaction(s) with von Willebrand $factor^+$ endothelial cells, $CD45^+$ blood-derived leucocytes and $f4/80^+$ phagocytes. Occasionally, $f4/80^+$ phagocytes being immunoreactive also for GFP were identified, thus

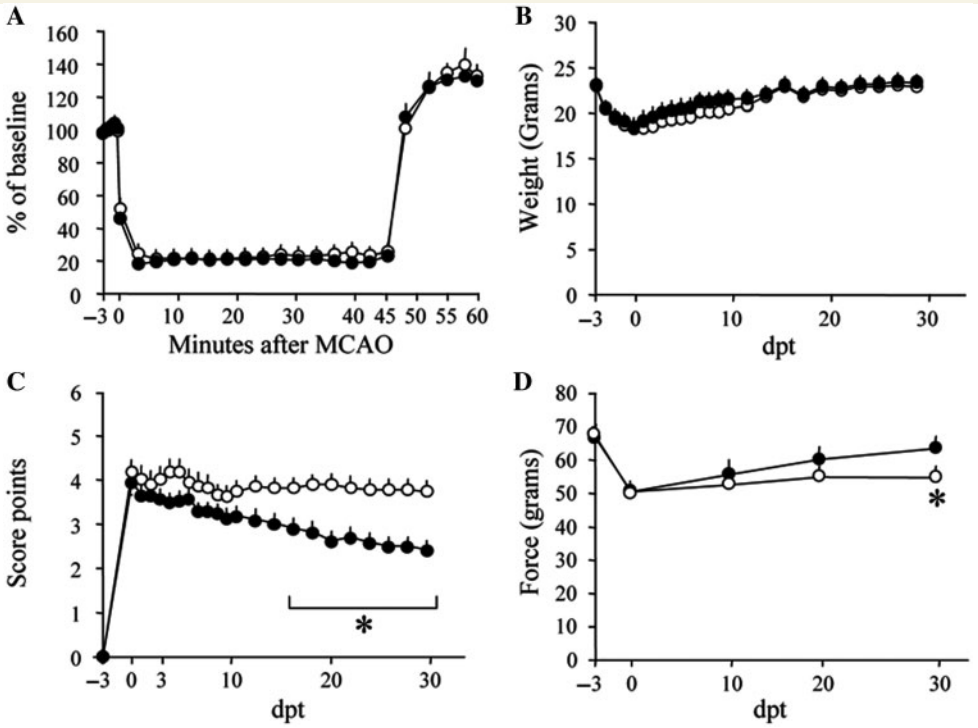

Figure 1 Amelioration of neurological deficits. (**A**) LDF recordings before (−3 to 0 min), during and after 45 min of intraluminal MCAO. No differences on LDF were noted before, during and after MCAO between the two groups. (**B**) Body weight in the 4 weeks following MCAO. No significant difference in body weight was ever observed between the two groups. (**C**) mNSS and (**D**) grip strength test, evaluated on the paretic right forepaw. Note the functional improvement in NPC-treated mice. Open circles in **A–D** refer to sham-treated mice, while filled circles refer to NPC-treated mice. Data are expressed as mean values ± SE. *$P \leqslant 0.05$, compared with sham-treated MCAO mice.

suggesting that only very low numbers of i.v.-injected NPCs might have been phagocytosed *in vivo* (Fig. 2G–H).

Few scattered GFP$^+$ NPCs were found in the spleen, liver, kidneys and lungs up to 30 dpt (Supplementary Fig. 2). No pathological signs suggestive of overt toxic effects (e.g. inflammation, necrosis, cell degeneration) were found in any of these organs.

Protection from delayed ischaemic injury and enhancement of neuronal survival

To understand how NPCs delivery improved functional recovery after stroke, we analysed the treatment effect on histopathological brain injury. Cresyl violet-based morphometrical analysis of brain swelling or atrophy showed no difference, when NPC-treated MCAO mice were compared with sham-treated controls at both 0, 3 and 10 dpt (Fig. 3A and C). In contrast, significant reduction of the lesion volume by 21.5% was detected at 30 dpt in NPC-treated mice ($P \leqslant 0.05$) (Fig. 3B–E). The regional analysis of the surviving tissue indicated that NPC effect on lesion size was due to a protection of residual striatal brain tissue (total striatal volume in the ischaemic hemisphere: sham treated, $1.99 \pm 0.20\,mm^3$; NPC treated, $2.59 \pm 0.20\,mm^3$, $P = 0.05$; 23% lesion volume reduction). The morphometric analysis of the surviving cortical tissue showed no significant difference between the groups.

The total lesion volume was found to be inversely correlated with grip strength at 30 dpt ($r = -0.877$, $r^2 = 0.769$; $P = 0.0002$), but not to the mNSS.

Modulation of inflammation-, astrogliosis- and neuronal survival-related genes at mRNA level

In order to elucidate the molecular mechanism(s) underlying the observed NPC-mediated protection from brain ischaemic injury progression, we next performed a wide TaqMan®-based semi-quantitative gene expression profiling in the two brain hemispheres (both ipsi- and contralateral to the stroke) from sham-treated and NPC-treated MCAO mice at 0, 3, 10 and 30 dpt.

Forty-five different mRNA species involved in angiogenesis, astrogliosis, inflammation and neuronal survival were measured in the brain. Significant and homogeneous downregulation of several mRNA species was observed between 3 and 30 dpt in NPC-treated MCAO mice, as shown by progressive decrease of the regression curve slope values (m) at 3 ($m = 1.15$), 10 ($m = 0.67$) and 30 dpt ($m = 0.57$), respectively. Further correlation index analysis on scatter plots revealed that differences in gene expression were mostly seen in the ischaemic hemispheres at

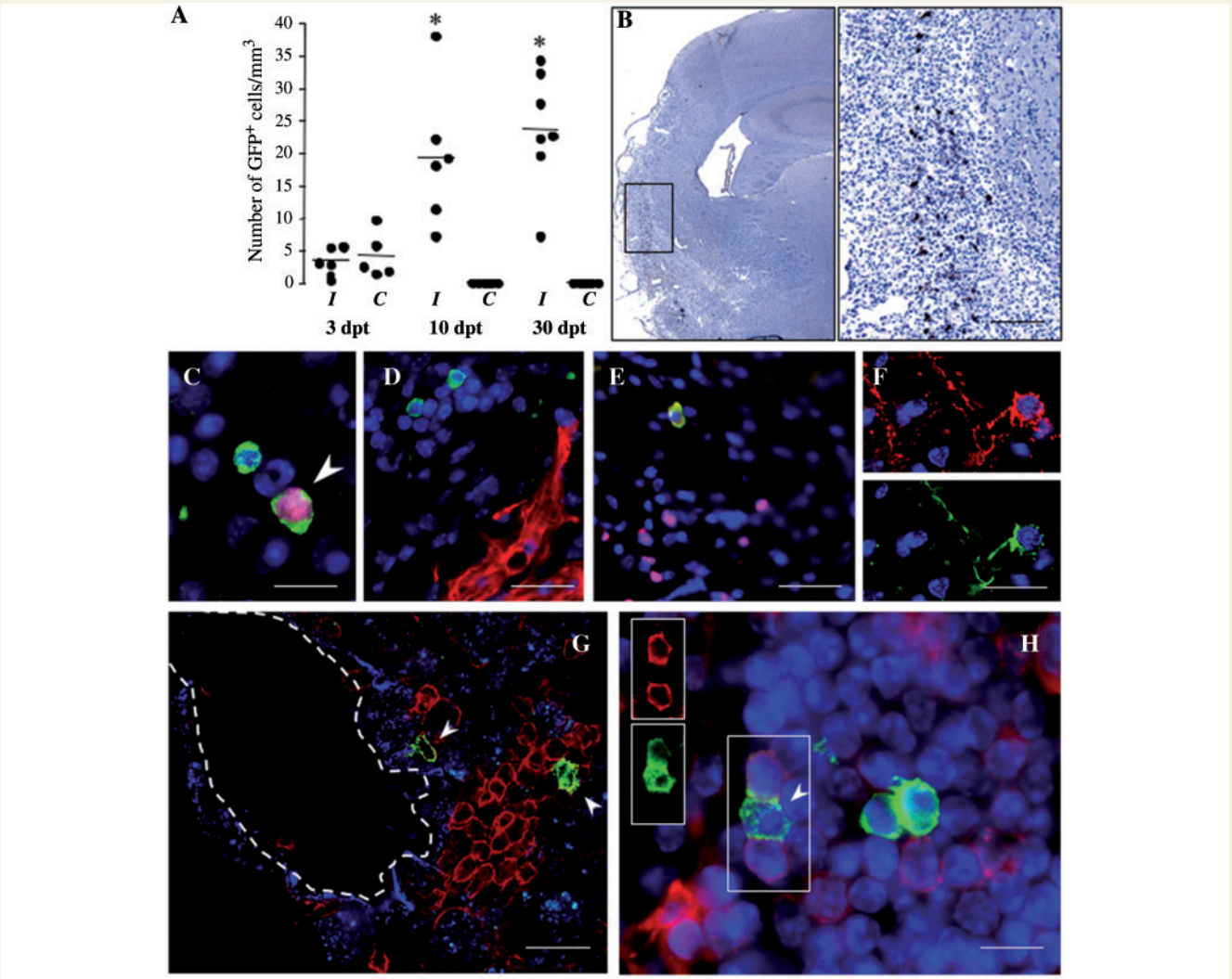

Figure 2 Accumulation and persistence of injected NPCs in the brain ischaemic boundary zone. (**A**) Quantification of the number of i.v.-injected NPCs accumulating in the ischaemic brain at 3, 10 or 30 dpt. Filled circles correspond to individual mice. *I* indicate ipsilateral to ischemia, while *C* indicates contralateral to ischemia. $*P \leqslant 0.05$, compared with sham-treated MCAO mice. (**B**) Low-magnification view of the ischaemic brain hemisphere showing a cluster of GFP^+ NPCs (in brown) within the lesion border zone beneath the hippocampus at 10 dpt. The right image is a magnification of the boxed area. Nuclei were counterstained with haematoxylin. (**C**) Consistent proportion of i.v.-injected NPCs in the brain ischaemic boundary zone at 3 dpt are $Ki67^+$ (arrowhead, red). (**D–F**) At 30 dpt, some of transplanted NPCs express the oligodendrocyte-specific transcription factor Olig2 (red in **E**) or the neuronal marker doublecortin (red in **F**). No co-expression of GFP with the astroglial marker GFAP (red in **D**) was found at any time-point. (**G** and **H**) NPCs (arrowheads) at the ischaemic boundary zone were often detected in close proximity to von Willebrand $factor^+$ endothelial cells (blue in **G**), $CD45^+$ blood-derived leukocytes (red in **G**) and $f4/80^+$ phagocytes (red in **H**). Occasionally, $f4/80^+$ phagocytes being immunoreactive also for GFP (arrowhead in **H**) were identified. The white dotted line in **G** represents a blood vessel. GFP^+ cells are green in **C–H**. Nuclei (labelled with DAPI) are in blue in **C–F** and **H**. Images in **F** and **G** are deconvolved projections optimized by using Delta Vision (Applied Precision) software. Scale bars: **B**, 200 μm; **C**, 40 μm; **D**, 80 μm; **E**, 60 μm; **F**, 100 μm; **E**, **G** and **H**, 40 μm.

10 dpt ($r^2 = 0.82$), when compared with 3 and 30 dpt ($r^2 = 0.96$ and 0.93, respectively) (Supplementary Fig. 3), which is notably significant before group differences in brain injury became evident. Interestingly, 42.2% (19/45) of the genes did not change at any time-point. Only 2.2% (1/45) of the genes were upregulated in NPC-treated mice at 3 dpt, among which we identified *DARPP-32* (1.7-fold) (Fig. 4A). On the other hand, 55.6% (25/45) of the genes were downregulated in NPC-treated mice. Among these, the most prominent were (i) inflammatory regulators [e.g. interferon (IFN)-γ at 3 dpt (0.4-fold, $P \leqslant 0.05$) and at 10 dpt (0.6-fold), tumour necrosis factor (TNF)-α (0.5-fold, $P \leqslant 0.05$) at 10 dpt, interleukin (IL)-1β (0.5-fold, $P \leqslant 0.05$), IL-6 (0.5-fold, $P \leqslant 0.05$) and leptin receptor (0.7-fold, $P = 0.07$) at 30 dpt]; (ii) regulators of (astro)glial proliferation and reactivity [e.g. fibroblast growth factor (FGF)-II (0.7-fold, $P \leqslant 0.01$) at 10 dpt, the marker of reactive astrocytes vimentin (0.4-fold, $P \leqslant 0.05$) (Galou *et al.*, 1996) at 30 dpt] and (iii) neuronal death and plasticity [e.g. the executioner caspase-3 (0.7-fold, $P \leqslant 0.05$) at 10 dpt, the growth-associated protein (GAP)-43 (0.6-fold, $P \leqslant 0.01$) and the chondroitin sulphate proteoglycan versican

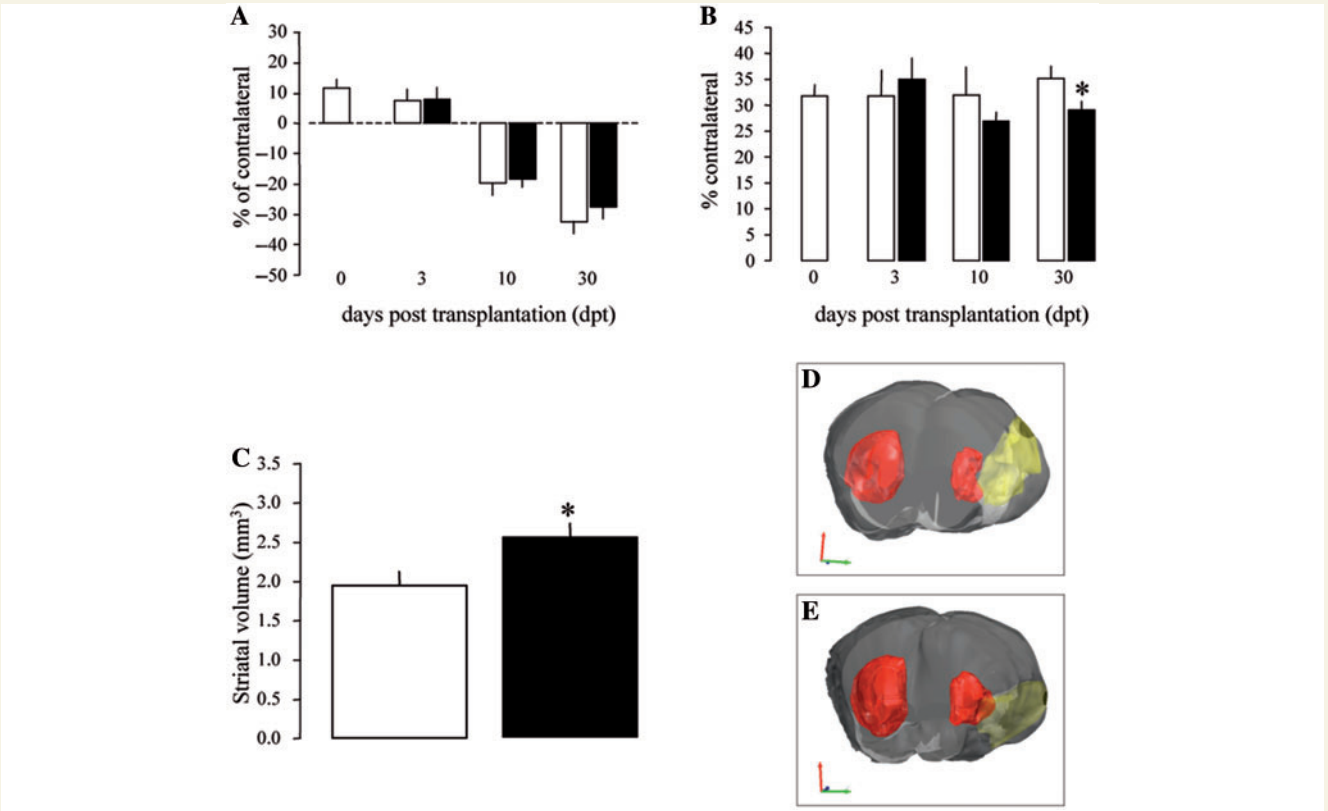

Figure 3 Protection from the progression of brain ischaemic injury. (**A**) Brain oedema/atrophy. Brain hemisphere volume ipsilateral to ischemia is maximal at 0 dpt. At 3 dpt the oedema decreases while a substantial degree of atrophy is observed at 10 dpt and it further progresses up to 30 dpt. (**B**) Evolution of the ischaemic lesion volume over time. (**C**) Spared striatal tissue volume of the ipsilateral hemisphere at 30 dpt as calculated from the analysis of serial sections for stereology-based counts. (**D** and **E**) Representative 3D reconstructions of the forebrain (grey), striatum (red) and ischaemic lesion (yellow) at 30 dpt of a representative sham-treated (**D**) and NPC-treated mice (**E**) obtained from the sequential sections ($n = 18$ sections per mouse) analysed for stereology. White bars refer to sham-treated MCAO mice, while black bars refer to NPC-treated MCAO mice. Data in **A**, **B** and **C** are expressed as means ± SE. *$P = 0.05$, compared with sham-treated MCAO mice.

(0.7-fold, $P = 0.059$) at 30 dpt] (Fig. 4). Genes involved in the angiogenic response to ischaemia (Hif-1α, KDR, EPO, Flt-1, VEGF-α) in the perilesional area changed only slightly after ischaemia and only subtle changes were observed between the two treatment groups. At 30 dpt, stereological-based estimates of the total density and length of capillaries in sham- and NPC-treated mice were not significantly different (total capillary density: $6.751 \times 10^{-4} \pm 3.978 \times 10^{-5}$ µm/µm^3 versus $6.682 \times 10^{-4} \pm 2.846 \times 10^{-5}$ µm/µm^3, $P = 0.890$; total length of capillaries: $1.732 \times 10^6 \pm 6.82 \times 10^5$ µm versus $2.20 \times 10^6 \pm 4.05 \times 10^5$ µm, $P = 0.163$, in sham and NPC-treated mice, respectively). In the contralateral non-ischaemic hemisphere, the large majority of mRNA species (29/45, 64.4%) remained unchanged. A comprehensive description of the gene expression data is shown in the Supplementary Table 1. These data indicate that the delayed i.v. injection of NPCs potently regulates the expression of several mRNA species in the ischaemic brain.

Attenuation of the inflammatory response

To further characterize the effects of NPC transplantation on the local inflammatory response, we analysed morphometrically the total brain area stained with the common leucocyte antigen CD45 as well as the density of microglial cells in the ischaemic boundary zone both at 3, 10 and 30 dpt.

While NPC-treated mice showed a significant reduction of both CD45$^+$ and ionized calcium binding adaptor molecule 1 (IBA-1$^+$) cells at 30 dpt only (both $P \leqslant 0.05$, when compared with sham-treated controls) (Fig. 5A–C and G), a significant reduction of IBA-1$^+$/major histocompatibility complex class II molecule (MHC-II$^+$) cells was observed at both 3 and 10 dpt (both $P \leqslant 0.05$) (Fig. 5D–F).

Inhibition of (astro)glial scar formation

Gliotic scar formation is regarded as a major factor hampering recovery from stroke (Li *et al.*, 2005; Yiu and He, 2006). Thus, we next measured the area and thickness of the Glial fibrillary acidic protein (GFAP$^+$) glial scar wall in the infarct border zone (Fig. 6A). Again, NPC-treated mice showed a smaller scar area at 30 dpt ($P \leqslant 0.05$). When corrected for the border length profile irregularities, this also resulted in a significantly thinner scar ($P \leqslant 0.01$) (Fig. 6B–E), the difference among the two treatment

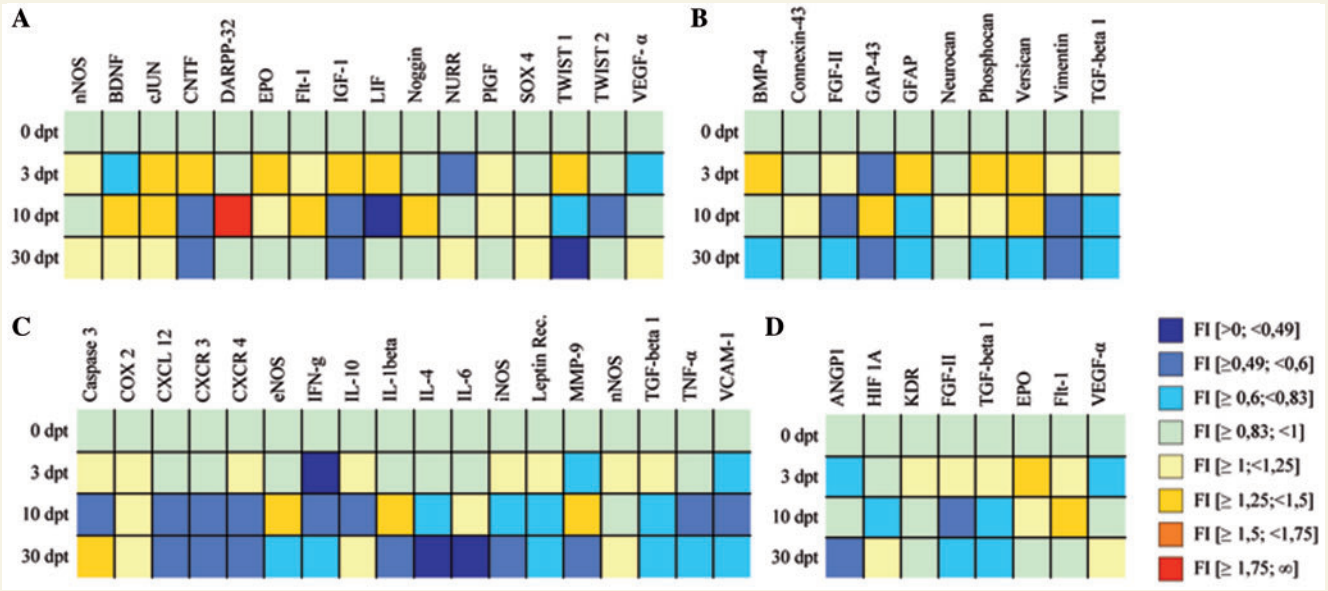

Figure 4 Modulation of inflammation, astrogliosis and neuronal survival at mRNA level. Semi-quantitative analysis of selected mRNAs in the brain of MCAO mice injected i.v. with NPCs. The colour-coded graphs depict the expression profile of a list of selected genes involved in neuronal survival (**A**), (astro)-gliosis (**B**), inflammation (**C**) and angiogenesis (**D**). Significant modulation of the genes in the brains of NPC-treated MCAO mice, when compared with sham-treated controls is observed. Data were determined in the ischaemic brain hemispheres (ipsilateral to the stroke) and are expressed as mean fold induction (F.I.) as compared with sham-treated mice. Upregulation may be assumed for values of F.I. $\geqslant 1.5$ and downregulation for values of F.I. $\leqslant 0.6$.

groups of mice was particularly evident at the rostrocaudal level of the bregma.

Promotion of neuronal survival

Further analysis showed that NPC-treated MCAO mice had higher densities of surviving neuronal nuclear antigen $(NeuN)^+$ neurons in the striatum ipsilateral to the stroke starting at 3 and 10 dpt, getting significant at 30 dpt, compared with sham-treated controls (Fig. 7A–C and Supplementary Fig. 4). No differences were seen in other structures, namely in the cortex, hippocampus and thalamus (data not shown). These findings were also substantiated with unbiased stereological counts (Fig. 7D–G). Furthermore, by applying the optical-fractionator methodology at tissues obtained at 30 dpt only, we observed significantly more Darpp-32^+ medium spiny neurons, as well as $D2R^+$ neurons (a subpopulation of medium spiny neurons) (Kawaguchi, 1997) (Fig. 7F and E, $P \leqslant 0.05$ and $P \leqslant 0.01$, respectively) in the striatum of NPC-treated ischaemic mice, when compared with sham-treated controls. Finally, though NPC-transplanted mice displayed a slightly higher number of $ChAT^+$ interneurons (a subpopulation of interneurons particular resistant to ischaemia) (Andsberg *et al*., 2001), the difference to sham-treated animals was not statistically significant ($P = 0.33$) (Fig. 7G).

The enhanced neuronal survival was also reflected by a significant reduction ($P \leqslant 0.05$) of the total number of apoptotic cells (in particular neurons) displaying either cleavage of caspase 3 (3 dpt) or DNA fragmentation (3 and 10 dpt) in the ischaemic hemisphere of NPC-treated MCAO mice, when compared with sham-treated controls (Fig. 8A and B, Supplementary Fig. 4).

Prevention of corpus callosum atrophy by NPCs

There is substantial evidence that ischaemic lesions may induce degeneration of long distance, interhemispheric projections (Napieralski *et al*., 1996), such as those crossing the corpus callosum (CC). Indeed, the quantification of the medial CC ipsilateral to the stroke revealed that NPC-treated ischaemic mice had a significantly thicker CC at 30 dpt, when compared with sham-treated controls ($P \leqslant 0.05$) (Fig. 8C). These latter data point towards a more successful remodelling of interhemispheric projections in NPC—as compared with sham-treated MCAO mice.

Discussion

In ischaemic stroke the time-window, in which survival promoting therapies are efficacious, is extremely limited. As such, recanalizing drugs (i.e. thrombolytics) (Busch *et al*., 1998; Kilic *et al*., 2000; Hacke *et al*., 2008) as well as neuroprotective compounds [e.g. NMDA receptor antagonists (Ma *et al*., 1998), free radical scavengers (Yang *et al*., 2000), growth factors (Cerami, 2001) or caspase-3 inhibitors (Endres *et al*., 1998)] protect brain tissue only when delivered in the first 1–3 and in some conditions up to 6 h after stroke. That the therapeutic window is so narrow has been explained by the fact that brain infarct evolves very rapidly, typically within a few hours up to 3–4 days after stroke, depending on the duration and severity of ischaemia (Garcia *et al*., 1993; Namura *et al*., 1998; Hata *et al*., 2000; Li *et al*., 2000; Hermann *et al*., 2001). In case of ischaemias exhibiting a severity that is close to the threshold at which brain infarcts develop, some

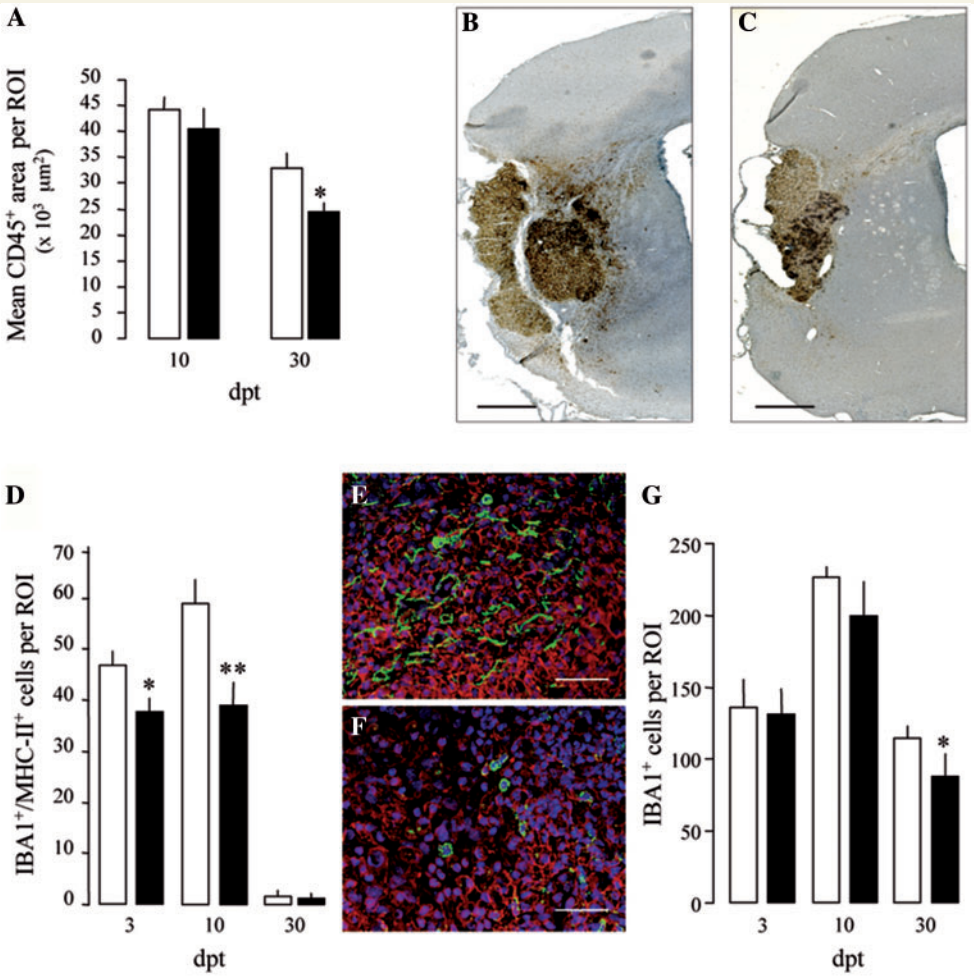

Figure 5 Reduction of the inflammatory reaction. (**A**) Quantitative analysis of the CD45$^+$ leukocyte infiltrate area in the peri-ischaemic boundary zone. (**B** and **C**) Low-power images showing the infiltration of CD45$^+$ cells (brown) in the hemisphere ipsilateral to the stroke in a representative sham- (**B**) and NPC-treated (**C**) mice. Nuclei were counterstained with haematoxylin. (**D**) Quantitative analysis of the IBA-1$^+$/MHC-II$^+$ activated microglia reaction at 3, 10 and 30 dpt. (**E** and **F**) Deconvolved projections of MHC-II (green) immune-reactivity IBA-1$^+$ (red) microglial cells in the hemisphere ipsilateral to the stroke in representative sham-(**E**) and NPC- (**F**) treated MCAO mice at 10 dpt. Nuclei are in blue (DAPI). (**G**) Quantitative analysis of IBA-1$^+$ macrophages/microglia in the peri-ischaemic boundary zone. White bars in **A**, **D** and **G** refer to sham-treated mice, while black bars refer to NPC-treated MCAO mice. Scale bars: **B** and **C**, 1 mm; **E** and **F**, 40 µm. Data in **A**, **D** and **G** are expressed as mean values ± SE. $*P \leqslant 0.05$, $**P \leqslant 0.01$ compared with sham-treated MCAO mice.

continued injury has also been reported outside that time-window period, i.e. up to 1 week after the ischaemia (Du *et al*., 1996; Snider *et al*., 1999; Hermann *et al*., 2001; Zheng *et al*., 2003; Guadagno *et al*., 2008). Whether this delayed injury is relevant for the final functional outcome of stroke remained unclear.

Using a broad set of behavioural neurological, histopathological, immunohistochemical and molecular biological techniques, we have characterized the effects of adult syngenic NPCs i.v.-administered 72 h after reperfusion (i.e. in delayed delivery approach) in MCAO mice. We show that NPCs are capable of integrating into the stroke brain—although at a low percentage (up to 0.28%)—where they are able to survive at least for 30 dpt. As such, the large majority of transplanted cells remained mainly in an undifferentiated state throughout the observation period. This resulted in a hitherto unreported very delayed structural neuroprotective effect, which we attribute to a protracted anti-inflammatory effect, occurring soon after cell transplantation but persisting up to 30 dpt, paralleled by a glial scar-inhibitory effect. Therefore, our data exemplify that neural differentiation is not a pre-requisite for adult NPCs to exert their restorative action thus representing an attractive tool for stroke treatment.

That NPCs integrate into the stroke brain has been shown previously (Bliss *et al*., 2007; Bacigaluppi *et al*., 2008). In contrast to the healthy brain, in which intraparenchymally transplanted NPCs migrate only over small distances and in small numbers, the ischaemic brain tissue fosters a selective NPC migration towards the stroke lesion where they eventually differentiate into functional neural cells (Kelly *et al*., 2004; Buhnemann *et al*., 2006; Darsalia *et al*., 2007). Whether robust cell replacement is

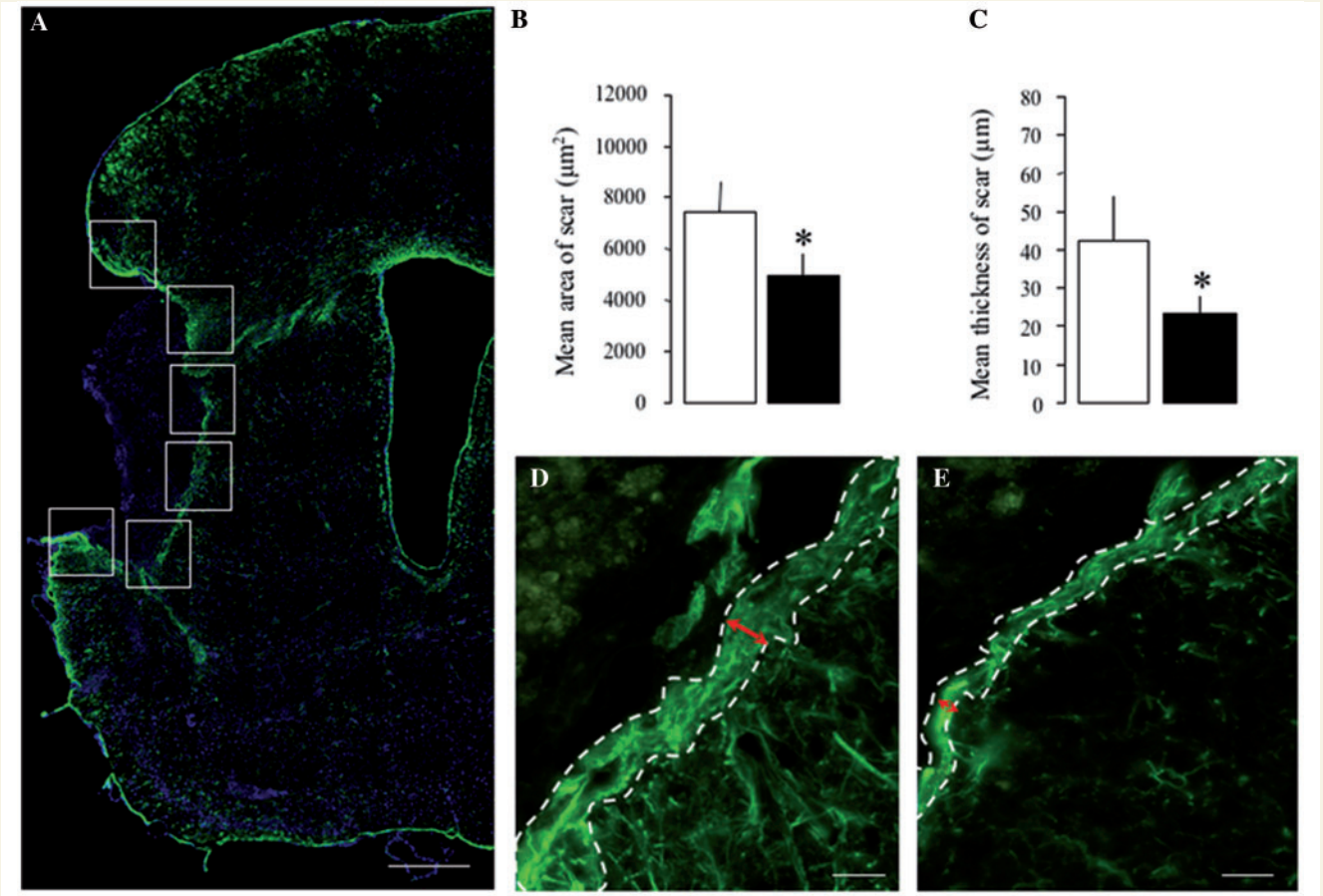

Figure 6 Reduction of astroglial scar formation. Quantitative analysis of the GFAP$^+$ astroglial scar area (**A**) and thickness (**B**) along the ischaemic border zone. White bars refer to sham-treated MCAO mice, while black bars refer to NPC-treated MCAO mice. Data in **B** and **C** are expressed as mean values and have been obtained from a total of six regions of interest, as shown by the white boxes in **A**. GFAP$^+$ astroglial scar thickness (red double arrow) in the hemisphere ipsilateral to the stroke in representative sham- (**D**) and NPC- (**E**) treated MCAO mice at 30 dpt. The white-dashed line outlines the astroglial scar. The green staining in **A**, **D** and **E** is for GFAP. Scale bars: **A**, 1 mm, **D** and **E**, 20 μm. Data are means ± SE. *$P \leqslant 0.05$, compared with sham-treated mice.

indeed responsible for the functional improvement induced by NPCs was recently challenged by studies using i.v. transplantation strategies. Early evidence showed a substantial integration and differentiation of i.v.-injected human- or embryonic-neural stem cells into neurons and astrocytes in rodents with experimental intracerebral haemorrhage or focal cerebral ischaemia (Jeong *et al*., 2003; Jin *et al*., 2005). Indeed, more recent studies have identified an additional bystander immune-modulatory mechanism, sustained and mediated by i.v.-injected NPC, that is capable of ameliorating clinico-pathological signs of experimental bacterial collagenase VII-induced intracerebral haemorrhage (Lee *et al*., 2008). This latter mechanism is considered one of the main mechanisms by which systemically injected NPCs exert their therapeutic effects in chronic and acute inflammatory CNS diseases (the concept of 'therapeutic plasticity') (Martino and Pluchino, 2006).

In our study, anti-inflammatory and glial scar-inhibitory effects might be common mechanistic pathways through which transplanted NPCs protected the ischaemic brain from delayed injury. The anti-inflammatory mechanism in NPC-transplanted mice is supported by the observed reduction of mRNA levels of pro-inflammatory mediators (i.e. IFN-γ, TNF-α, IL-1β and IL-6) (Barone *et al*., 1997; Hallenbeck, 2002; Allan *et al*., 2005) that contribute to the detrimental post-ischaemic brain inflammation in the lesioned areas of transplanted mice and also by the decreased number of activated microglial cells. This latter evidence, recorded soon after cell transplantation, was further reinforced by the reduction of blood-borne CNS-infiltrating inflammatory cells (CD45$^+$) at 30 dpt. Further, a glial scar-inhibitory effect in NPC-transplanted mice takes place as suggested by the downregulation of genes promoting astrogliosis (e.g. FGF-II, transforming growth factor-beta (TGF-β), vimentin) in the lesioned area that was accompanied by a statistically significant reduction of the perilesional glial scar thickness at 30 dpt. Although we did observe a slight but non-significant increase of the total length of capillaries, vessel density was not altered after NPC treatment. We favour this as the *in vivo* proof that NPC treatment did not induce an angiogenic response. The larger volume of spared striatal in NPC-treated animals can, in fact, explain the increase total length values.

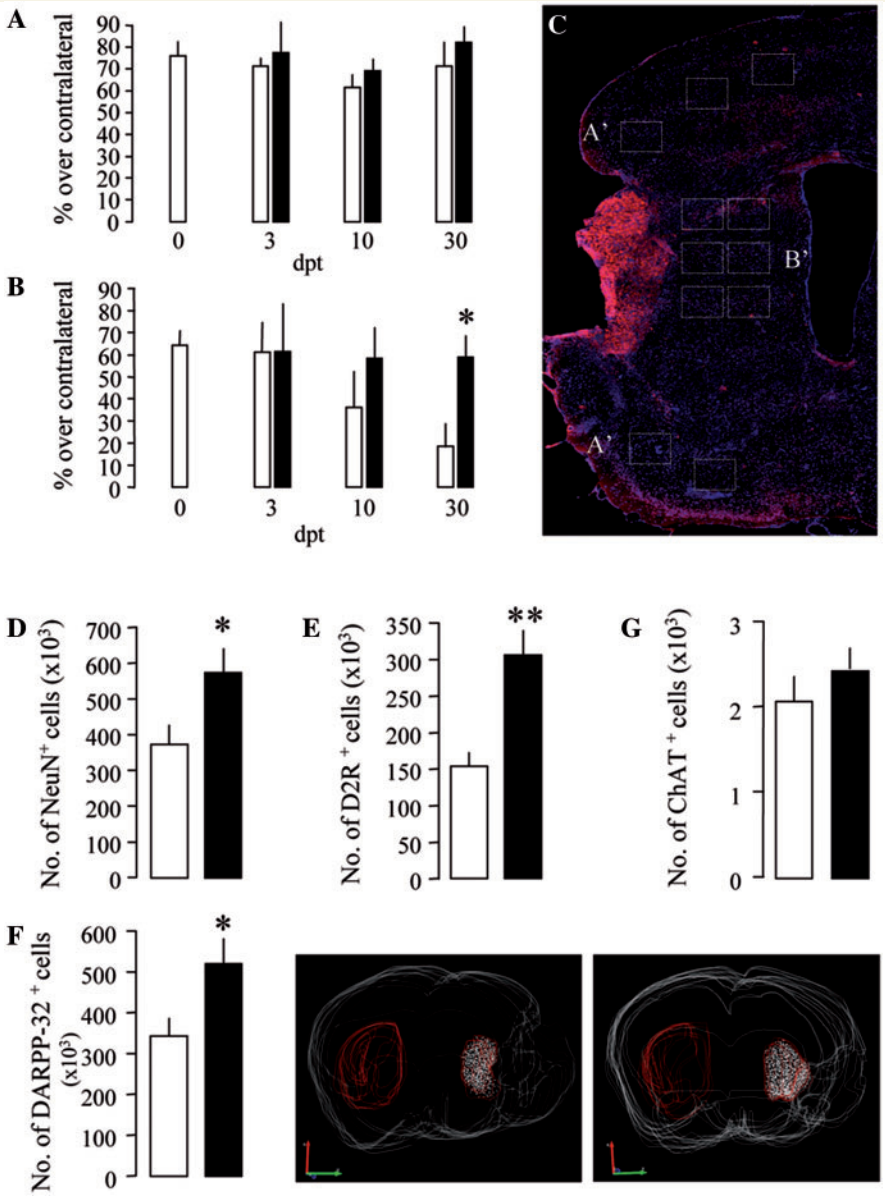

Figure 7 Support of neuronal survival. Neuronal survival in the cortex (**A**) and striatum (**B**) ipsilateral to the stroke. Data are expressed as percentage of NeuN$^+$ cells (over contralateral hemisphere). (**C**) Representative staining for NeuN (red) of the ischaemic hemisphere at 30 dpt. White boxes indicate the five cortical (*a*) and six striatal (*b*) fields selected for cell countings shown in **A** and **B**. Absolute numbers of NeuN$^+$ (**D**), D2-Receptor$^+$ (**E**), Darpp-32$^+$ (**F**) and ChAT$^+$ (**G**) neurons in the total unlesioned striatum of the ischaemic hemisphere quantified using the method for unbiased stereological counting of cells based on the optical fractionator method. 3D reconstructions in (**F**) from two representative sham- and NPC-treated mice (left and right, respectively) showing surviving Darpp-32$^+$ cells in the hemisphere ipsilateral to the lesion. White bars refer to sham-treated MCAO mice, while black bars refer to NPC-treated MCAO mice. Data are means ± SE. *$P \leqslant 0.05$, **$P \leqslant 0.01$ compared with sham-treated mice.

Finally, we cannot exclude that the anti-inflammatory effects exerted in MCAO mice transplanted with NPCs is in part exerted in the body periphery, as recently shown after brain haemorrhage (Lee *et al*., 2008). However, we found that soon after MCAO (e.g. 3 dpt) a comparable number of blood-borne inflammatory cells infiltrated the CNS, thus indicating that the recruitment of 'effector' immune cells from the periphery was not impaired by the cell treatment and, again, suggesting that the protective effect may have been induced within the CNS.

By providing a detailed temporospatial analysis, our data show that focal cerebral ischaemia is followed by delayed neurodegenerative process that continues over >10 dpt, i.e. 13 days after the stroke, resulting in continuous neuronal loss in those parts of the striatum that survived the ischaemic insult, leading to secondary lesion growth. In our study, post-acute NPC treatment provided a delayed structural neuroprotective effect—particularly evident on striatal medium spiny neurons—despite the fact that treatment was initiated far beyond established time-windows

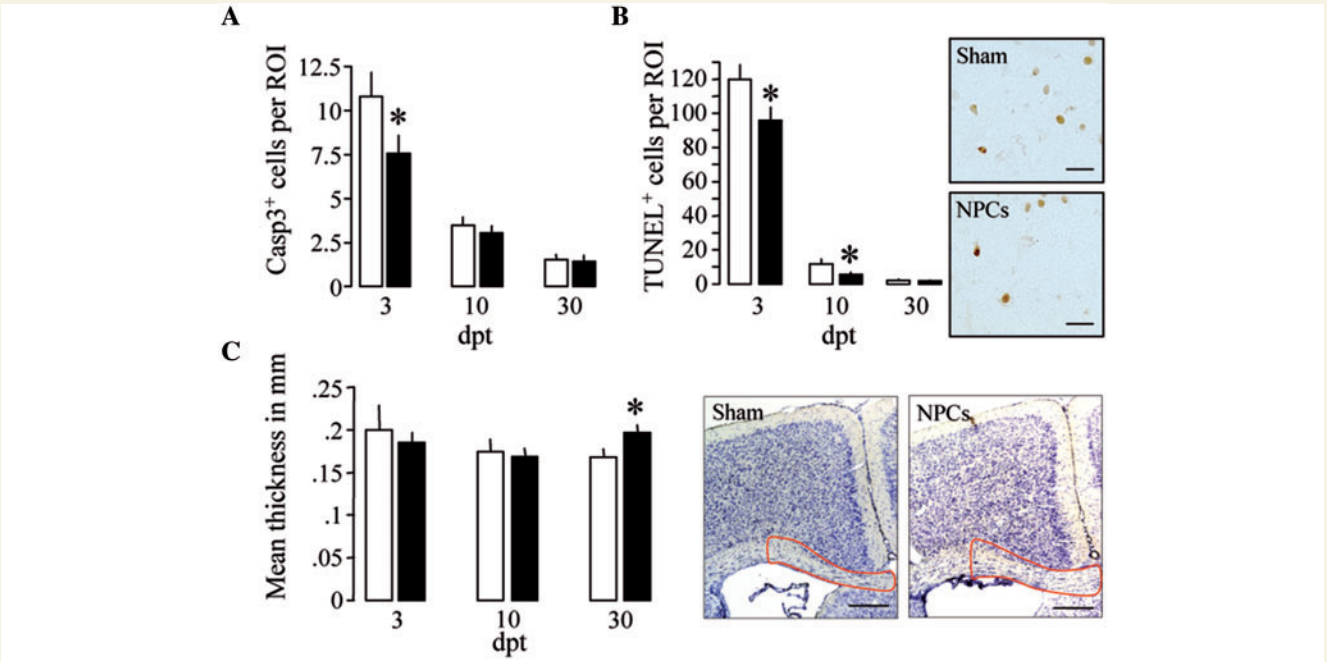

Figure 8 Reduction of apoptosis and of CC atrophy. Quantitative analysis of activated caspase 3^+ (**A**) and Terminal deoxynucleotidyl transferase dUTP nick end labeling ($TUNEL^+$) cells (**B**) in the ischaemic hemisphere and representative images for $TUNEL^+$ cells in sham- and NPC-treated mice at 3 dpt. (**C**) Cresyl violet-based quantification of the CC thickness at 30 dpt. The red line in the microphotographs refers to the measured area of the CC. White bars refer to sham-treated MCAO mice, while black bars refer to NPC-treated MCAO mice. Scale bar: 40 μm (**B**) and 300 μm (**C**). Data are means ± SE. $*P \leqslant 0.05$, compared with sham-treated mice.

for neuroprotection. We tend to attribute this late effect to the early anti-inflammatory effect we observed.

A significant downregulation of TNF-α, a known pro-inflammatory cytokine exerting a profound pro-apoptotic effect (Kaushal and Schlichter, 2008), was observed in the striatum of NPC-treated mice. Downregulation of IFN-γ is also worth mentioning. It has been shown that IFN-γ is able to induce apoptosis by increasing expression of death receptor on target cells (Furlan *et al*., 2001; Hallenbeck, 2002). Considering that neuronal cells do express death receptors such as tumour necrosis factor receptor-1 (TNFR1) (Haase *et al*., 2008), it is tempting to speculate that the reduction of IFN-γ secretion within the lesioned area might contribute *per se* to the pro-survival neuronal effect. Further, the importance of both TNF-α and IFN-γ is emphasized by the demonstration that antagonization of the production of either of these inflammatory cytokines significantly prevented secondary infarct growth after stroke (Liesz *et al*., 2009). The reduction of expression of genes coding for cell death molecules (e.g. caspase-3) in transplanted mice would further support this view.

This immune-modulatory, rather than immune-suppressive action exerted by NPCs may be of pivotal interest as stroke is accompanied by an early peripheral immunodeficiency phase (Meisel *et al*., 2005; Offner *et al*., 2006; Offner *et al*., 2009) that limits the application of systemic immunosuppressive therapies.

Our data exemplify that delayed structural injury indeed exists after ischaemic stroke, and that this injury can be partially reversed by NPC transplantation leading to clinically relevant functional neurological improvements. As these structural changes were observed in a time-window in which remodelling and plasticity processes are very active in the tissue, our data question whether delayed degeneration and remodelling should indeed be regarded as distinct phenomena. Indeed, it has previously been shown that successful remodelling is accompanied by structural changes both in ischaemic tissue and remote from it. As such, remodelling of axonal fibre bundles (Jiang *et al*., 2006) associated with an increase in the thickness of the CC (Shen *et al*., 2006) has been reported in stroke animals exhibiting enhanced motor recovery after treatment with bone marrow cells. Yet in this study, the structural changes seen were interpreted as consequence of delayed neuroprotection rather than post-acute plasticity.

In conclusion, our data support the concept that transplanted NPCs, remaining undifferentiated, might promote recovery from ischaemic injury via a multifaceted therapeutic response. This is preferentially exerted through an anti-inflammatory effect that leads to decreased glia scar formation and protects the brain from delayed injury. Based on our here-presented results, cell-based strategies may particularly be attractive for this kind of tissue injury.

Supplementary material

Supplementary material is available at *Brain* online.

Acknowledgements

We acknowledge the assistance and help of Miriam Ascagni, Cesare Covino, Angela Fendel, Filippo Martinelli Boneschi and Annett Spudich.

Funding

NCCR ''Neural plasticity'' (to D.M.H.); COST Short Term Scientific Mission (COST-STSM-BM0603-2843); the Swiss National Science Foundation (3200B0-112056/1, to D.M.H.); the BMW Italy Group (to G.M.); Banca Agricola Popolare di Ragusa (to S.P.).

References

Allan SM, Tyrrell PJ, Rothwell NJ. Interleukin-1 and neuronal injury. Nat Rev Immunol 2005; 5: 629–40.

Andsberg G, Kokaia Z, Lindvall O. Upregulation of p75 neurotrophin receptor after stroke in mice does not contribute to differential vulnerability of striatal neurons. Exp Neurol 2001; 169: 351–63.

Bacigaluppi M, Pluchino S, Martino G, Kilic E, Hermann DM. Neural stem/precursor cells for the treatment of ischaemic stroke. J Neurol Sci 2008; 265: 73–7.

Barone FC, Arvin B, White RF, Miller A, Webb CL, Willette RN, et al. Tumor necrosis factor-alpha. A mediator of focal ischaemic brain injury. Stroke 1997; 28: 1233–44.

Bliss T, Guzman R, Daadi M, Steinberg GK. Cell transplantation therapy for stroke. Stroke 2007; 38: 817–26.

Buhnemann C, Scholz A, Bernreuther C, Malik CY, Braun H, Schachner M, et al. Neuronal differentiation of transplanted embryonic stem cell-derived precursors in stroke lesions of adult rats. Brain 2006; 129: 3238–48.

Busch E, Kruger K, Allegrini PR, Kerskens CM, Gyngell ML, Hoehn-Berlage M, et al. Reperfusion after thrombolytic therapy of embolic stroke in the rat: magnetic resonance and biochemical imaging. J Cereb Blood Flow Metab 1998; 18: 407–18.

Cerami A. Beyond erythropoiesis: novel applications for recombinant human erythropoietin. Semin Hematol 2001; 38: 33–9.

Darsalia V, Kallur T, Kokaia Z. Survival, migration and neuronal differentiation of human fetal striatal and cortical neural stem cells grafted in stroke-damaged rat striatum. Eur J Neurosci 2007; 26: 605–14.

Dirnagl U, Iadecola C, Moskowitz MA. Pathobiology of ischaemic stroke: an integrated view. Trends Neurosci 1999; 22: 391–7.

Du C, Hu R, Csernansky CA, Hsu CY, Choi DW. Very delayed infarction after mild focal cerebral ischemia: a role for apoptosis? J Cereb Blood Flow Metab 1996; 16: 195–201.

Endres M, Namura S, Shimizu-Sasamata M, Waeber C, Zhang L, Gomez-Isla T, et al. Attenuation of delayed neuronal death after mild focal ischemia in mice by inhibition of the caspase family. J Cereb Blood Flow Metab 1998; 18: 238–47.

Fawcett JW, Asher RA. The glial scar and central nervous system repair. Brain Res Bull 1999; 49: 377–91.

Furlan R, Brambilla E, Ruffini F, Poliani PL, Bergami A, Marconi PC, et al. Intrathecal delivery of IFN-gamma protects C57BL/6 mice from chronic-progressive experimental autoimmune encephalomyelitis by increasing apoptosis of central nervous system-infiltrating lymphocytes. J Immunol 2001; 167: 1821–9.

Galou M, Colucci-Guyon E, Ensergueix D, Ridet JL, Gimenez y Ribotta M, Privat A, et al. Disrupted glial fibrillary acidic protein network in astrocytes from vimentin knockout mice. J Cell Biol 1996; 133: 853–63.

Garcia JH, Yoshida Y, Chen H, Li Y, Zhang ZG, Lian J, et al. Progression from ischaemic injury to infarct following middle cerebral artery occlusion in the rat. Am J Pathol 1993; 142: 623–35.

Guadagno JV, Jones PS, Aigbirhio FI, Wang D, Fryer TD, Day DJ, et al. Selective neuronal loss in rescued penumbra relates to initial hypoperfusion. Brain 2008; 131: 2666–78.

Haase G, Pettmann B, Raoul C, Henderson CE. Signaling by death receptors in the nervous system. Curr Opin Neurobiol 2008; 18: 284–91.

Hacke W, Kaste M, Bluhmki E, Brozman M, Davalos A, Guidetti D, et al. Thrombolysis with alteplase 3 to 4.5 hours after acute ischaemic stroke. N Engl J Med 2008; 359: 1317–29.

Hallenbeck JM. The many faces of tumor necrosis factor in stroke. Nat Med 2002; 8: 1363–8.

Hata R, Maeda K, Hermann D, Mies G, Hossmann KA. Evolution of brain infarction after transient focal cerebral ischemia in mice. J Cereb Blood Flow Metab 2000; 20: 937–46.

Hermann DM, Kilic E, Hata R, Hossmann KA, Mies G. Relationship between metabolic dysfunctions, gene responses and delayed cell death after mild focal cerebral ischemia in mice. Neuroscience 2001; 104: 947–55.

Hossmann KA. Pathophysiology and therapy of experimental stroke. Cell Mol Neurobiol 2006; 26: 1057–83.

Jeong SW, Chu K, Jung KH, Kim SU, Kim M, Roh JK. Human neural stem cell transplantation promotes functional recovery in rats with experimental intracerebral hemorrhage. Stroke 2003; 34: 2258–63.

Jiang Q, Zhang ZG, Ding GL, Silver B, Zhang L, Meng H, et al. MRI detects white matter reorganization after neural progenitor cell treatment of stroke. Neuroimage 2006; 32: 1080–9.

Jin K, Sun Y, Xie L, Mao XO, Childs J, Peel A, et al. Comparison of ischemia-directed migration of neural precursor cells after intrastriatal, intraventricular, or intravenous transplantation in the rat. Neurobiol Dis 2005; 18: 366–74.

Karimi-Abdolrezaee S, Eftekharpour E, Wang J, Morshead CM, Fehlings MG. Delayed transplantation of adult neural precursor cells promotes remyelination and functional neurological recovery after spinal cord injury. J Neurosci 2006; 26: 3377–89.

Kaushal V, Schlichter LC. Mechanisms of microglia-mediated neurotoxicity in a new model of the stroke penumbra. J Neurosci 2008; 28: 2221–30.

Kawaguchi Y. Neostriatal cell subtypes and their functional roles. Neurosci Res 1997; 27: 1–8.

Kelly S, Bliss TM, Shah AK, Sun GH, Ma M, Foo WC, et al. Transplanted human fetal neural stem cells survive, migrate, and differentiate in ischaemic rat cerebral cortex. Proc Natl Acad Sci USA 2004; 101: 11839–44.

Kilic E, Hermann DM, Hossmann KA. Recombinant tissue-plasminogen activator-induced thrombolysis after cerebral thromboembolism in mice. Acta Neuropathol 2000; 99: 219–22.

Lee JP, Jeyakumar M, Gonzalez R, Takahashi H, Lee PJ, Baek RC, et al. Stem cells act through multiple mechanisms to benefit mice with neurodegenerative metabolic disease. Nat Med 2007; 13: 439–47.

Lee ST, Chu K, Jung KH, Kim SJ, Kim DH, Kang KM, et al. Anti-inflammatory mechanism of intravascular neural stem cell transplantation in haemorrhagic stroke. Brain 2008; 131: 616–29.

Li F, Silva MD, Sotak CH, Fisher M. Temporal evolution of ischaemic injury evaluated with diffusion-, perfusion-, and T2-weighted MRI. Neurology 2000; 54: 689–96.

Li Y, Chen J, Zhang CL, Wang L, Lu D, Katakowski M, et al. Gliosis and brain remodeling after treatment of stroke in rats with marrow stromal cells. Glia 2005; 49: 407–17.

Liesz A, Suri-Payer E, Veltkamp C, Doerr H, Sommer C, Rivest S, et al. Regulatory T cells are key cerebroprotective immunomodulators in acute experimental stroke. Nat Med 2009; 15: 192–9.

Ma J, Endres M, Moskowitz MA. Synergistic effects of caspase inhibitors and MK-801 in brain injury after transient focal cerebral ischaemia in mice. Br J Pharmacol 1998; 124: 756–62.

Martino G, Pluchino S. The therapeutic potential of neural stem cells. Nat Rev Neurosci 2006; 7: 395–406.

Meisel C, Schwab JM, Prass K, Meisel A, Dirnagl U. Central nervous system injury-induced immune deficiency syndrome. Nat Rev Neurosci 2005; 6: 775–86.

Mouton PR, Gokhale AM, Ward NL, West MJ. Stereological length estimation using spherical probes. J Microsc 2002; 206: 54–64.

Namura S, Zhu J, Fink K, Endres M, Srinivasan A, Tomaselli KJ, et al. Activation and cleavage of caspase-3 in apoptosis induced by experimental cerebral ischemia. J Neurosci 1998; 18: 3659–68.

Napieralski JA, Butler AK, Chesselet MF. Anatomical and functional evidence for lesion-specific sprouting of corticostriatal input in the adult rat. J Comp Neurol 1996; 373: 484–97.

Nedergaard M, Dirnagl U. Role of glial cells in cerebral ischemia. Glia 2005; 50: 281–6.

Nudo RJ. Recovery after damage to motor cortical areas. Curr Opin Neurobiol 1999; 9: 740–7.

Offner H, Subramanian S, Parker SM, Wang C, Afentoulis ME, Lewis A, et al. Splenic atrophy in experimental stroke is accompanied by increased regulatory T cells and circulating macrophages. J Immunol 2006; 176: 6523–31.

Offner H, Vandenbark AA, Hurn PD. Effect of experimental stroke on peripheral immunity: CNS ischemia induces profound immunosuppression. Neuroscience 2009; 158: 1098–111.

Pluchino S, Quattrini A, Brambilla E, Gritti A, Salani G, Dina G, et al. Injection of adult neurospheres induces recovery in a chronic model of multiple sclerosis. Nature 2003; 422: 688–94.

Pluchino S, Zanotti L, Rossi B, Brambilla E, Ottoboni L, Salani G, et al. Neurosphere-derived multipotent precursors promote neuroprotection by an immunomodulatory mechanism. Nature 2005; 436: 266–71.

Shen LH, Li Y, Chen J, Zhang J, Vanguri P, Borneman J, et al. Intracarotid transplantation of bone marrow stromal cells increases axon-myelin remodeling after stroke. Neuroscience 2006; 137: 393–9.

Snider BJ, Gottron FJ, Choi DW. Apoptosis and necrosis in cerebrovascular disease. Ann N Y Acad Sci 1999; 893: 243–53.

West MJ, Slomianka L, Gundersen HJ. Unbiased stereological estimation of the total number of neurons in the subdivisions of the rat hippocampus using the optical fractionator. Anat Rec 1991; 231: 482–97.

Witte OW. Lesion-induced plasticity as a potential mechanism for recovery and rehabilitative training. Curr Opin Neurol 1998; 11: 655–62.

Yang Y, Li Q, Shuaib A. Neuroprotection by 2-h postischemia administration of two free radical scavengers, alpha-phenyl-n-tert-butyl-nitrone (PBN) and N-tert-butyl-(2-sulfophenyl)-nitrone (S-PBN), in rats subjected to focal embolic cerebral ischemia. Exp Neurol 2000; 163: 39–45.

Yiu G, He Z. Glial inhibition of CNS axon regeneration. Nat Rev Neurosci 2006; 7: 617–27.

Zheng Z, Zhao H, Steinberg GK, Yenari MA. Cellular and molecular events underlying ischemia-induced neuronal apoptosis. Drug News Perspect 2003; 16: 497–503.

Ziv Y, Avidan H, Pluchino S, Martino G, Schwartz M. Synergy between immune cells and adult neural stem/progenitor cells promotes functional recovery from spinal cord injury. Proc Natl Acad Sci USA 2006; 103: 13174–9.

Zivin JA. Factors determining the therapeutic window for stroke. Neurology 1998; 50: 599–603.